

## Crystal Structure and Thermodynamic Stability of the $[\text{Hg}(\text{Pyridine})_4(\text{NO}_3)_2] \cdot 2(\text{Pyridine})$ Inclusion Compound

V.YU. KOMAROV<sup>1</sup>, E.A. UKRAINTSEVA<sup>1</sup>, D.V. SOLDATOV<sup>1,2,\*</sup>, G.D. ENRIGHT<sup>2</sup>, P.S. GALKIN<sup>1</sup>, R. LUBORADZKI<sup>3</sup> and J. LIPKOWSKI<sup>3</sup>

<sup>1</sup>*Nikolaev Institute of Inorganic Chemistry, Siberian Branch of the Russian Academy of Sciences, Ac. Lavrent'ev Av. 3, Novosibirsk, 630090 Russia;* <sup>2</sup>*Steacie Institute for Molecular Sciences, National Research Council of Canada, 100 Sussex Dr., Ottawa, ON, Canada K1A 0R6;* <sup>3</sup>*Institute of Physical Chemistry, Polish Academy of Sciences, Kasprzaka 44/52, Warsaw, 01-224 Poland*

(Received: 19 February 2004; in final form: 10 May 2004)

**Key words:** crystal structure, mercury(II) nitrate, pyridine, tensimetric method, thermodynamic stability, Werner clathrates

### Abstract

The studied compound belongs to the family of  $[\text{MPy}_4\text{X}_2] \cdot 2\text{Py}$  isomorphous clathrates. Its crystal structure exhibits a van der Waals architecture formed by neutral  $[\text{HgPy}_4(\text{NO}_3)_2]$  host molecules, with the guest pyridine molecules included in the cavities of the host lattice. The host complex is formed by coordination of four pyridines, located near the equatorial plane, and two nitrates, located axially, to the Hg(II) cation. One of nitrates ligates as a monodentate ligand and another as a bidentate. The coordination polyhedron is 'HgN<sub>4</sub>O<sub>3</sub>', with average Hg—N<sub>Py</sub> and Hg—O<sub>nitrate</sub> distances of 2.38(5) and 2.68(1) Å, respectively. The crystal structure is complicated with a superlattice and the crystal symmetry reduced to monoclinic, as compared to the structure usually occurring in the  $[\text{MPy}_4\text{X}_2] \cdot 2\text{Py}$  clathrates. The pyridine vapor pressure over the clathrate was measured in the 293–369 K temperature range by the static tensimetric method. Thermodynamic parameters of the clathrate dissociation were calculated from these data. For the reaction  $1/3[\text{HgPy}_4(\text{NO}_3)_2] \cdot 2\text{Py}_{\text{solid}} = 1/3[\text{HgPy}_3(\text{NO}_3)_2]_{\text{solid}} + \text{Py}_{\text{gas}}$  the parameters are as follows:  $\Delta H_{\text{av}}^0 = 49.4(2)$  kJ/mol,  $\Delta S_{\text{av}}^0 = 127(2)$  J/(mol K) and  $\Delta G_{298}^0 = 11.4(3)$  kJ/mol. The results are compared with previously reported data on compounds of the  $[\text{MPy}_4(\text{NO}_3)_2] \cdot 2\text{Py}$  series.

### Introduction

Molecular metal complexes provide a countless library of tunable building units for the design of supramolecular materials [1–6]. A set of useful properties such materials may possess stimulates an increasing interest in the synthesis, structure and properties of the complexes [7–20]. Weak bonding among the building units in molecular materials creates advantages: allows for the variation of the units within the same type of material, facilitates the transient and reversible conversion from one structure to another, and makes the materials sensitive and responsive to external conditions [21]. At the same time, weak bonding creates problems for the purposeful design of such materials. Molecular self-assembly may proceed in various energetically similar architectures, with the resultant defined by a balance of several factors equally contributing to the overall stability of the structure. The determination of these factors is an important step in the prediction of

molecular and crystal structure of supramolecular materials as well as the prediction of the limits of their thermal and thermodynamic stability.

The general experimental approach we use for the above purposes is a combination of methods defining structure and stability of studied materials. A convenient choice for such studies is an isomorphous series of inclusion compounds. The parameters defining stability of the compounds are readily available from the studies of their thermal dissociation [22–24].

Our recent studies were focused on a family of Werner clathrates of general formula  $[\text{MPy}_4\text{X}_2] \cdot 2\text{Py}$  (Py = pyridine) with various metal(II) cations M and anionic ligands X in the host complex formulation [25–43]. The compounds exhibit the same basic architecture that is adjustable to the geometry of the host complex and survives guest replacement. The clathrates of the nitrate series,  $[\text{MPy}_4(\text{NO}_3)_2] \cdot 2\text{Py}$  (M = Mn, Co, Ni, Cu, Zn and Cd), form an isostructural series crystallizing in the orthorhombic *Ccca* space group (Table 1). Within this series, the thermal and thermodynamic stability of the clathrates follows the general stability sequence for

\* Author for correspondence. E-mail: soldatov@che.nsk.su

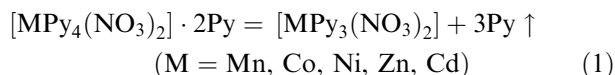
Table 1. Crystal structure types and melting points of known  $[\text{MPy}_4(\text{NO}_3)_2] \cdot 2\text{Py}$  clathrates, and  $\Delta G_{298}^\circ$  of their dissociation according to the equation:  $1/3[\text{MPy}_4(\text{NO}_3)_2] \cdot 2\text{Py}_{\text{solid}} = 1/3[\text{MPy}_3(\text{NO}_3)_2]_{\text{solid}} + \text{Py}_{\text{gas}}$

M	Space group ( <i>T</i> -range)	M.p. (K)	$\Delta G_{298}^\circ$ (kJ/mol)	Ref.
Mn	<i>Ccca</i> (up to 354 K)	354	11.4(5)	[34, 40, 43]
Co	<i>Ccca</i> (up to 361 K)	361	12.8(2)	[27, 40, 43]
Ni	<i>Ccca</i> (lower 347 K)	381	14.4(6)	[26, 40, 43]
Cu	<i>Ccca</i> (higher 319 K)	418	16.7(6) <sup>a</sup>	[41, 40, 43]
	<i>Pnna</i> <sup>b</sup> (lower 319 K)		17.9(6) <sup>a</sup>	
Zn	<i>Ccca</i> (up to 335 K)	335	11.1(9)	[29, 43]
Cd	<i>Ccca</i> (higher 221 K)	379	12.5(5)	[33, 30, 40]
	<i>Pcca</i> <sup>b</sup> (lower 221 K)			

<sup>a</sup>The Cu compound dissociates in two steps; given value refers to a sum of two dissociation reactions normalized to one mole of releasing pyridine [40, 43].

<sup>b</sup>Isomorphous with the orthorhombic (*Ccca*) type [41, 33].

metal complexes (Mn < Co < Ni < Cu > Zn), [43] that is the strength of the host complex is a factor defining stability limits of the clathrate phases. In all cases except Cu, the individual host complexes are not sufficiently stable to form solvent-free materials [25, 29, 30, 40]. For instance, the dissociation of the clathrates in air or under vacuum occurs according to the following equation:



The  $[\text{MPy}_4(\text{NO}_3)_2]$  complex molecules are stabilized in the clathrate matrix and, therefore, the isolation of clathrate compounds is a convenient, and may be the only, method to observe and to characterize such tetrapyrindine complexes.

The compound of this study was isolated as a white crystalline solid of gross formula  $[\text{Hg}(\text{NO}_3)_2 \cdot 6\text{Py}]$ . The similarity of the product to known  $[\text{MPy}_4(\text{NO}_3)_2] \cdot 2\text{Py}$  clathrates, containing only terminally coordinated nitrates, was questionable as previously reported  $\text{Hg}(\text{II})$  complexes have nitrate coordinated to the metal cation either as a bidentate or as a bridging ligand [44–56]. Nevertheless, our preliminary studies [57] led to a surprising conclusion that the title compound belongs to the  $[\text{MPy}_4(\text{NO}_3)_2] \cdot 2\text{Py}$  clathrate series. Further similarity to the series was observed in thermal dissociation behavior of the compound which showed the loss of three moles of pyridine in a single step [57]. In this work we report crystal structure of the title clathrate, molecular structure of the  $[\text{HgPy}_4(\text{NO}_3)_2]$  complex which never was isolated as a solvent-free compound, pyridine vapor pressure over the title clathrate as a function of temperature, and thermodynamic parameters of dissociation of the clathrate. Finally, we compare structural and thermodynamic data on the entire  $[\text{MPy}_4(\text{NO}_3)_2] \cdot 2\text{Py}$  series.

## Experimental

### Preparations

The title clathrate was prepared in two steps. The slow addition of pyridine (2 mL, 25 mmol) to the stirred aqueous solution (50 mL) of  $\text{Hg}(\text{NO}_3)_2 \cdot \text{H}_2\text{O}$  (3.4 g, 10 mmol) acidified with several drops of  $\text{HNO}_3$  resulted in a white precipitate. The reaction mixture was dried in a draft and recrystallized from hot pyridine to give a bulk white crystalline product. Yield on Hg was ~65%. Hg content was determined by titration with EDTA, using eriochrome black T as an indicator. Found: Hg, 25.4(7)%. Calcd. for  $[\text{HgPy}_4(\text{NO}_3)_2] \cdot 2\text{Py}$ : Hg, 25.1%. The crystals were kept in a desiccator in dry pyridine atmosphere; in air they decomposed showing a loss corresponding to three moles of pyridine.

### Vapor pressure measurements

The pyridine vapor pressure over the clathrate was measured in the 293–369 K temperature range by the static tensimetric method using Pyrex membrane spoon-type null-manometers [58, 59]. The experimental set-up has been previously described [23]. The sensitivity of the membranes varied within 0.03–0.1 Torr (1 Torr = 1 mm Hg = 133.32 Pa). The temperature of the reaction vessel containing the sample was maintained with a water thermostat within 0.05 K. The reaction vessel was loaded with 0.8 g sample of the clathrate in a dry box, evacuated and sealed. The pressure–temperature dependence was reversible and reproducible in both forward and backward directions of the dissociation reaction. The equilibrium was reached in several hours or faster.

### Single-crystal XRD experiments

Single crystals of the title compound were studied on a Nonius Kappa-CCD X-ray diffractometer (MoK<sub>α</sub> radiation,  $\lambda = 0.71073 \text{ \AA}$ , graphite monochromator) equipped with an Oxford CryoSystem low-temperature device. All experiments were run at 150 K to prevent guest loss. The integration of the diffraction profiles and an empirical absorption correction utilized the standard set of programs associated with the diffractometer [60, 61]. The unit cell parameters were calculated from the entire data set. In spite of the proximity of all angles to 90°, the monoclinic cell was chosen after comparing the agreement between equivalents for the possible Laue groups. The structure was solved and refined in  $P2_1/n$  space group using the SHELXTL package [62]. The structural refinement was performed on  $F^2$  and applied to all data with positive intensities. Non-hydrogen atoms were refined anisotropically. The refinement suggested full occupancy for the guest pyridine within standard deviation of 1%; in the final solution the occupancy was fixed to an ideal value. In other words, the occupancy factors of all guest molecules were

assembled to be 100%. Most solution problems were caused by a large size of the unit cell and proximity of the monoclinic angle to 90°. An initial solution revealed instability and left large residual extrema of  $\sim 5 \text{ e}/\text{\AA}^3$ . Further refinement based on a twinning model resulted in a satisfactory final solution with reasonable residual extrema of  $-1.76$  and  $+1.82 \text{ e}/\text{\AA}^3$  located near the Hg atoms. The crystal was a pseudo-merohedric twin; the refinement was performed with the TWIN instruction (TWIN matrix: 1 0 0 0  $-1$  0 0 0  $-1$ ) in the SHELXTL suite of programs [62]. The minor fraction of the twin component was 0.260(1). For two other crystals randomly chosen and independently studied the values were 0.308(1) and 0.454(1).

A summary of crystal data and experimental parameters is given in Table 2. Selected geometric parameters for the structure are listed in Table 3. Further details and complete structural information have been deposited with the Cambridge Crystallographic Data Centre as CCDC 230577.

## Results and discussion

### Crystal structure

The present study confirms the inclusion character of the compound and its formulation as  $[\text{HgPy}_4$

Table 2. Single-crystal XRD analysis: crystal data and experimental parameters

Compound	$[\text{HgPy}_4(\text{NO}_3)_2] \cdot 2\text{Py}$
Chemical formula	$\text{C}_{20}\text{H}_{20}\text{HgN}_6\text{O}_6, 2(\text{C}_5\text{H}_5\text{N})$
Formula weight	799.2
Temperature of study (K)	150
Crystal system	Monoclinic
Space group	$P2_1/n$
Unit cell dimensions	
$a$ (Å)	12.189(2)
$b$ (Å)	34.295(5)
$c$ (Å)	29.934(4)
$\beta$ (°)	90.02(1)
$V$ (Å <sup>3</sup> )	12513(3)
$Z$	16
$D_{\text{calc}}$ (g cm <sup>-3</sup> )	1.697
$\mu$ (MoK $\alpha$ ) (cm <sup>-1</sup> )	49.8
Crystal color and shape	White truncated octahedron
Crystal sizes (mm)	0.2 0.2 0.2
Total collected data	148826
Unique data [ $R_{\text{int}}$ ]	32322 [0.057]
Intense data ( $I > 2\sigma(I)$ )	21229
Refined parameters	1622
Goodness of fit on $F^2$	1.052
$R^a$ (intense data)	0.043
$R$ (all data)	0.082
Residual extrema (e Å <sup>-3</sup> )	$-1.76$ and $+1.82$
Twin fractions	0.740(1) and 0.260(1)
CCDC deposition number	230577

<sup>a</sup>  $R = \sum ||F_o| - |F_c|| / \sum |F_o|$ .

Table 3. Structural and conformational parameters of four crystallographically inequivalent host molecules in the  $[\text{HgPy}_4(\text{NO}_3)_2] \cdot 2\text{Py}$  clathrate (distances (Å), valent and dihedral angles (°),  $x$  is the number of the molecule)

	Molecule 1	Molecule 2	Molecule 3	Molecule 4
<i>Distances</i>				
Hg( $x$ )—N( $x1$ )	2.190(5)	2.195(5)	2.197(5)	2.194(5)
Hg( $x$ )—N( $x2$ )	2.552(6)	2.587(6)	2.581(6)	2.556(7)
Hg( $x$ )—N( $x3$ )	2.200(5)	2.189(5)	2.188(5)	2.189(5)
Hg( $x$ )—N( $x4$ )	2.556(6)	2.575(7)	2.561(6)	2.582(6)
Hg( $x$ )—O( $x51$ )	2.610(5)	2.675(6)	2.716(5)	2.661(6)
Hg( $x$ )—O( $x52$ )	2.775(5)	2.688(6)	2.666(5)	2.685(5)
Hg( $x$ )—O( $x61$ )	2.664(5)	2.673(5)	2.672(5)	2.699(6)
<i>Valent angles<sup>a</sup></i>				
N( $x1$ )—Hg( $x$ )—N( $x2$ )	85.4	86.7	85.8	86.4
N( $x2$ )—Hg( $x$ )—N( $x3$ )	94.4	93.3	94.3	93.4
N( $x3$ )—Hg( $x$ )—N( $x4$ )	89.2	89.9	89.2	89.8
N( $x4$ )—Hg( $x$ )—N( $x1$ )	89.2	88.0	88.9	88.4
N( $x1$ )—Hg( $x$ )—N( $x3$ )	172.5	172.0	172.8	172.7
N( $x2$ )—Hg( $x$ )—N( $x4$ )	164.6	164.4	164.4	164.1
O( $x51$ )—Hg( $x$ )—N( $x1$ )	100.9	102.2	100.7	101.6
O( $x51$ )—Hg( $x$ )—N( $x2$ )	75.9	75.8	75.0	75.8
O( $x51$ )—Hg( $x$ )—N( $x3$ )	86.3	85.5	86.2	85.4
O( $x51$ )—Hg( $x$ )—N( $x4$ )	119.4	119.7	120.4	120.0
O( $x52$ )—Hg( $x$ )—N( $x1$ )	85.6	86.5	86.4	85.1
O( $x52$ )—Hg( $x$ )—N( $x2$ )	118.6	119.5	118.8	119.0
O( $x52$ )—Hg( $x$ )—N( $x3$ )	101.0	100.5	99.8	101.2
O( $x52$ )—Hg( $x$ )—N( $x4$ )	75.3	74.7	75.4	75.4
O( $x61$ )—Hg( $x$ )—N( $x1$ )	93.2	92.5	92.8	92.9
O( $x61$ )—Hg( $x$ )—N( $x2$ )	83.2	82.5	82.7	83.3
O( $x61$ )—Hg( $x$ )—N( $x3$ )	79.4	79.5	80.1	79.8
O( $x61$ )—Hg( $x$ )—N( $x4$ )	82.6	83.1	82.9	82.0
<i>Dihedral angles<sup>b</sup></i>				
(eqt)-(Py1)	54.9	53.6	52.1	52.3
(eqt)-(Py2)	69.4	68.7	69.3	68.6
(eqt)-(Py3)	51.8	52.0	54.2	51.5
(eqt)-(Py4)	58.8	59.2	58.6	59.1
(eqt)-(nitrate1)	89.1	88.5	89.1	88.8
(eqt)-(nitrate2)	51.3	50.7	51.1	50.9
(eqt)-(ab)	4.5	4.4	4.9	4.7

<sup>a</sup> Standard deviations 0.2°.

<sup>b</sup> Standard deviations  $\sim 0.2^\circ$ . Least-squares planes are defined as follows: (eqt) – Hg( $x$ ), N( $x1$ ), N( $x2$ ), N( $x3$ ), N( $x4$ ); (Py1) – N( $x1$ ), C( $x11$ )-C( $x16$ ); (Py2), (Py3), and (Py4) are defined similar to (Py1); (nitrate1) – N( $x5$ ), O( $x51$ )-O( $x53$ ); (nitrate2) – N( $x6$ ), O( $x61$ )-O( $x63$ ); (ab) is (001) crystallographic plane.

$(\text{NO}_3)_2] \cdot 2\text{Py}$ . The structure comprises neutral molecules of two types assembled in a crystal by van der Waals forces. The compound is isomorphous with other clathrates of the  $[\text{MPy}_4(\text{NO}_3)_2] \cdot 2\text{Py}$  series [26, 27, 31, 33–36, 38]. At the same time, there are significant changes both in molecular structure of the host complex and in crystal packing.

The structure of the host molecule is illustrated in Figure 1. Four crystallographically distinct host molecules have similar structure and geometry (Table 3). The central Hg(II) cation is surrounded by seven donor atoms to give a ‘ $\text{HgN}_4\text{O}_3$ ’ polyhedron. The four N atoms,

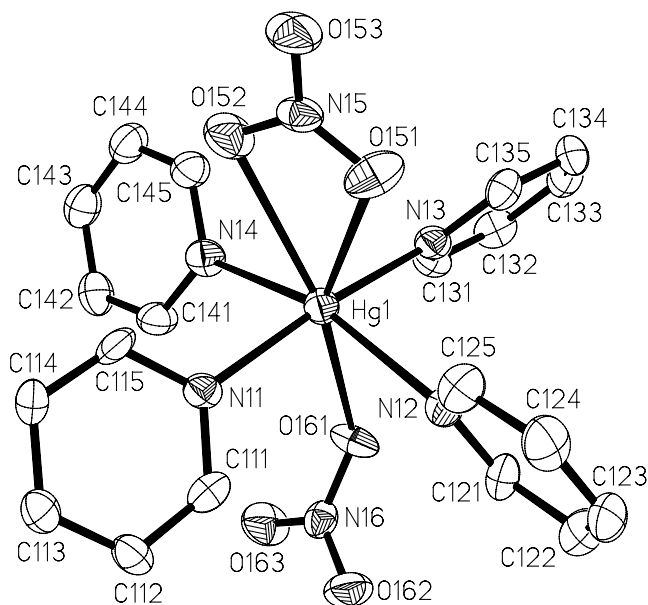


Figure 1. The host molecule in  $[\text{HgPy}_4(\text{NO}_3)_2] \cdot 2\text{Py}$  with atomic numbering scheme. The thermal ellipsoids are drawn at the 50% probability level; H atoms are omitted.

situated in the equatorial plane, arise from four pyridines rotating out of the plane to adopt a propeller conformation. Two nitrate anions ligate axially. The first nitrate is situated almost perpendicular to the equatorial plane in axial position and coordinates the Hg(II) cation in a bidentate fashion. This is an upside down position with respect to that observed in the previously studied  $[\text{MPy}_4(\text{NO}_3)_2] \cdot 2\text{Py}$  clathrates. The two Hg—O bonds are almost equivalent at distances within 2.6–2.8 Å. The second nitrate bends forward to the equatorial plane to form a dihedral angle of  $\sim 50^\circ$  with the plane; it coordinates to the Hg(II) cation in a monodentate fashion, with the Hg—O distance of  $\sim 2.7$  Å. The observed positioning of the nitrate groups favors the formation of weak hydrogen bonds [63] between O atoms of the groups and ortho-hydrogens of pyridine ligands. For the molecule shown in Figure 1 these bonds are characterized by the following inter-atomic distances (the corresponding H—C $\cdots$ O angles are given in brackets): O(151) $\cdots$ C(125), 3.05 Å (119°); O(151) $\cdots$ C(135), 3.13 Å (132°); O(152) $\cdots$ C(115), 3.17 Å (135°); O(152) $\cdots$ C(145), 3.13 Å (114°); O(161) $\cdots$ C(131), 3.01 Å (114°).

In previously studied  $[\text{MPy}_4(\text{NO}_3)_2] \cdot 2\text{Py}$  clathrates, the host molecules exhibit octahedral ‘trans-MN<sub>4</sub>O<sub>2</sub>’ polyhedra. The formation of the host species with two monodentate nitrates rather than formation of hexapyridine  $[\text{MPy}_6]^{2+}$  cations was understood to be a result of unfavorable repulsive interactions between pyridines upon coordination of six pyridine ligands to the metal cation [36]. This factor is likely to be less important for Hg(II). The Hg(II) cation is larger than the previously studied cations, and the coordination bonds are 0.2–0.7 Å longer, with average Hg—N<sub>Py</sub> and Hg—O<sub>nitrate</sub> distances of 2.38(5) and 2.68(1) Å, respectively.

In another similar complex,  $[\text{HgPy}_3(\text{CF}_3\text{COO})_2]$ , where the Hg(II) cation is surrounded by seven donor atoms (‘HgN<sub>3</sub>O<sub>4</sub>’), the average Hg—N<sub>Py</sub> and Hg—O<sub>trifluoroacetate</sub> distances are 2.31(5) and 2.68(6) Å, respectively [64]. In  $[\text{HgPy}_6](\text{CF}_3\text{SO}_3)_2$ , the Hg(II) cation is octahedrally coordinated by six N atoms from six pyridines with the average Hg—N distance of 2.45(2) Å [65]. In a structure containing complex anion  $[\text{Hg}(\text{NO}_3)_4]^{2-}$ , the Hg(II) cation is surrounded by eight O atoms from four bidentate nitrates with average Hg—O<sub>nitrate</sub> distance of 2.44(5) Å [56]. As may be seen from the above comparison, coordination of Hg(II) by six, seven or eight donor atoms, including coordination by six pyridines or four bidentate nitrates, is possible, without significant effect on the average strength of the coordination bond. Therefore, the realization of the  $[\text{HgPy}_4(\text{NO}_3)_2]$  species should be defined by some factors other than impossibility of the hexapyridine coordination. One of the factors is likely to be a favorable packing of the species in the clathrate phase, while bulky hexapyridine cations having lower conformational freedom may be difficult to pack effectively. The hexapyridine complex cations may form in such cases as  $[\text{HgPy}_6](\text{CF}_3\text{SO}_3)_2$ , where the anion is too large to support the clathrate architecture. Another factor may be the formation of an extra coordination bond by the bidentate nitrate because an additional bond would be impossible in a hexapyridine complex.

The crystal packing in the clathrate of this study is shown in Figure 2a. The guest pyridine molecules occupy cavities formed by nitrate and pyridine fragments of the host. The cavities are combined to form rectangular channels stretching along the *a* crystallographic direction. It is quite unusual that dramatic changes in the host molecule, especially the coordination mode of the nitrates, still lead to the architectural type observed for earlier studied  $[\text{MPy}_4(\text{NO}_3)_2] \cdot 2\text{Py}$  compounds (Figure 2b) [26, 27, 31, 33–36, 38]. As compared to  $[\text{NiPy}_4(\text{NO}_3)_2] \cdot 2\text{Py}$ , the title compound has doubled *b* and *c* parameters yielding a four times larger unit cell, and the crystal symmetry is reduced to monoclinic. Although the four crystallographically distinct host molecules have similar conformations, their centers are displaced by 0.51–0.55 Å from the positions they would have in the smaller orthorhombic cell. This factor and the inequivalency of two nitrate ligands result in eight cavities which slightly differ in shape. Guest molecules adjust their orientations according to the spatial requirements, with the angle between their planes and the (*bc*) crystallographic plane ranging within 53.9°–60.2°. It should be noted that all guest molecules are well ordered and their dipoles are nearly parallel to the *b* axis and alternate along the channel running along the *a* axis.

#### Thermodynamic stability

The experimental data showing equilibrium pyridine vapor pressure over the clathrate versus temperature are

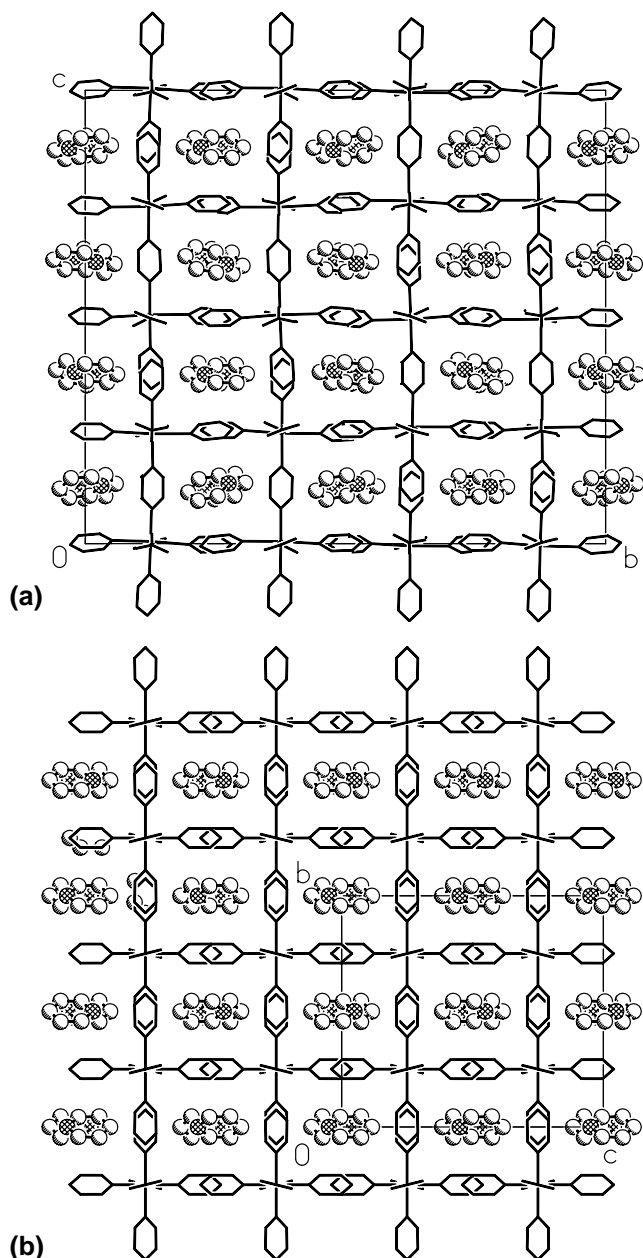


Figure 2. A comparison of crystal packing in the studied  $[\text{HgPy}_4(\text{NO}_3)_2] \cdot 2\text{Py}$  compound (a) and in the  $[\text{NiPy}_4(\text{NO}_3)_2] \cdot 2\text{Py}$  compound [26] (b). Both structures are projected along the direction of the channels. The host molecules are displayed in wire-frame style and the guest molecules as ball and stick; H atoms are omitted.

illustrated in Figure 3. At room temperature the pyridine vapor pressure is significant at 7.7 Torr (cf. 20 Torr over neat pyridine) that accounts for fast dissociation of

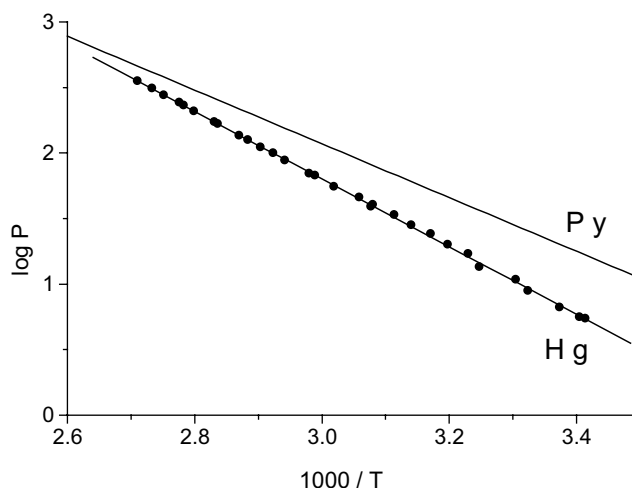


Figure 3. The pyridine vapor pressure over the  $[\text{HgPy}_4(\text{NO}_3)_2] \cdot 2\text{Py}$  compound versus temperature. The experimental data are presented in the  $\log P-1000/T$  coordinates ( $P$ , Torr;  $T$ , K). The dependence for pyridine vapor pressure over liquid pyridine is shown for comparison.

the compound in air. The temperature dependence is well approximated by the equation:

$$\log P = (9.54 \pm 0.03) - (2580 \pm 10)/T \quad (293-369 \text{ K}; 30 \text{ experimental points}) \quad (2)$$

The linearity of the dependence in the  $\log P-1000/T$  coordinates shows that the clathrate exists and experiences a single-type dissociation process in the whole temperature range studied. As found previously [57], the stoichiometry of the reaction is similar to that found for Zn, Cd and other analogues (cf. Equation 1):



The enthalpy, entropy and standard isobaric-isothermal potential of the dissociation, calculated from the dependence (2), are given in Table 4. The comparison of the thermodynamic parameters for the Zn, Cd and Hg compounds reveals that overall stability ( $\Delta G_{298}^0$ ) of the clathrates is similar. Closer consideration reveals systematic decrease in both the enthalpy and entropy components in the Zn, Cd, Hg series, that is their changing in a compensative manner. Such a trend is consistent with an increasing size of the cavity with increasing size of the host complex. The guest molecule experiences more freedom and less favorable contacts with atoms of the host in a looser cavity of the Hg

Table 4. A comparison of thermodynamic parameters of the dissociation reaction  $1/3[\text{MPy}_4(\text{NO}_3)_2] \cdot 2\text{Py}_{\text{solid}} = 1/3[\text{MPy}_3(\text{NO}_3)_2]_{\text{solid}} + \text{Py}_{\text{gas}}$  for selected  $[\text{MPy}_4(\text{NO}_3)_2] \cdot 2\text{Py}$  clathrates

M	T-range (K)	$\Delta H_{\text{av}}$ (kJ/mol)	$\Delta S_{\text{av}}^0$ (J/(mol K))	$\Delta G_{298}^0$ (kJ/mol)	Ref.
Zn	300–335	58.3(7)	158(2)	11.1(9)	[43]
Cd	290–360	54.9(3)	142(1)	12.5(5)	[30, 40]
Hg	293–369	49.4(2)	127(2)	11.4(3)	This work

compound that results in the smaller entropy and enthalpy changes upon guest release.

It is necessary to note that the dissociation reaction (3) includes not only releasing the guest pyridine into the gaseous phase but also releasing one pyridine initially bonded in the host complex. In case of first row transition metal cations the overall stability of the clathrate phases (Table 1) correlated with the strength of coordination bonds in the host complex. In case of the Zn, Cd, Hg series (Table 4) all three clathrates have similar  $\Delta G_{298}^0$  values and might have similar strength of the coordination bonds in the host complex.

## Conclusion

Structural studies on the family of the  $[\text{MPy}_4\text{X}_2] \cdot 2\text{Py}$  clathrates have shown that the same crystal architecture persistently forms with a wide variation of the host (M, X) components and replacement of the guest pyridine. In case of the nitrate series,  $[\text{MPy}_4(\text{NO}_3)_2] \cdot 2\text{Py}$ , the clathrate architecture forms even though most  $[\text{MPy}_4(\text{NO}_3)_2]$  host complexes do not exist in a solvent-free form. These studies have now been extended to the Hg(II) nitrate complex, with similar structure and properties observed for the title  $[\text{HgPy}_4(\text{NO}_3)_2] \cdot 2\text{Py}$  clathrate.

The Hg(II) cation is the largest of the M(II) cations employed to date. As a consequence, the studied compound shows significant structural distinctions. First, the molecular structure of the host complex is unusual due to the bidentate nitrate and the subsequent coordination environment of Hg(II) by seven donor atoms. Second, the crystal structure of the clathrate reveals a superlattice with a unit cell four times larger than usually observed, with the crystal symmetry reduced to monoclinic. The formation of the superstructure appears to be a consequence of increased size and irregular geometry of the host complex. In the usual orthorhombic (*Ccca*) structure the cavities would be too large for guest pyridine. Besides, orthorhombic symmetry would be unlikely due to the chemical inequivalency of nitrates.

Our thermodynamic studies on the clathrates utilize the variation of a single component in a series of similar compounds which undergo the same dissociation reaction yielding similar products. The  $[\text{MPy}_4\text{X}_2] \cdot 2\text{Py}$  clathrates is a good choice for such studies. Previously we studied several series: with variation of first row transition metal(II) cations, with different X ligands, and with various guests [40,43]. In this study we complete a new series, with variation of group 12 M(II) cations – Zn, Cd, Hg. The Hg(II) cation is the heaviest of M(II) cations employed to date and, in many respects, creates an extreme case in the family of  $[\text{MPy}_4\text{X}_2] \cdot 2\text{Py}$  clathrates. At the same time, our thermodynamic results indicate that even such a significant change of the host complex results in a bulk

material as energetically favorable as the other members of the series.

## Acknowledgements

This work was carried out within the scope of a collaborative program between the Nikolaev Institute of Inorganic Chemistry, Siberian Branch of the Russian Academy of Sciences and the Institute of Physical Chemistry, Polish Academy of Sciences. The authors thank Dr. S.F. Solodovnikov (Nikolaev Institute of Inorganic Chemistry) for valuable comments on the XRD studies accomplished in this work.

## References

1. J. Lipkowski: In J.L. Atwood, J.E.D. Davies, and D.D. MacNicol (eds.), *Inclusion Compounds*, Vol. 1, Academic Press, London (1984), pp. 59–103.
2. J. Hanotier and P. Radtitzky: In J.L. Atwood, J.E.D. Davies, and D.D. MacNicol (eds.), *Inclusion Compounds*, Vol. 1, Academic Press, London (1984), pp. 104–134.
3. J.S. Miller and A.J. Epstein: *Angew. Chem. Int. Ed. Engl.* **33**, 385 (1994).
4. M.P. Byrn, C.J. Curtis, Y. Hsiou, S.I. Khan, P.A. Sawin, A. Terzis, and C.E. Strouse: In D.D. MacNicol, F. Toda, and R. Bishop (eds.), *Comprehensive Supramolecular Chemistry*, Vol. 6, Pergamon, Oxford (1996).
5. I. Goldberg: *Chem. Eur. J.* **6**, 3863 (2000).
6. K. Araki and H.E. Toma: *Quim. Nova* **25**, 962 (2002).
7. M.J. Hardie and C.L. Raston: *Chem. Commun.* 1153 (1999).
8. M. Albrecht, M. Lutz, A.L. Spek, and G. Koten: *Nature* **406**, 970 (2000).
9. Z. Olejnik, T. Lis, A. Vogt, S. Wolowicz, and J. Skarzewski: *J. Inclusion Phenom.* **38**, 221 (2000).
10. C. Karunakaran, K.R.J. Tomas, A. Asurname, and R. Murugesan: *J. Inclusion Phenom.* **38**, 233 (2000).
11. D.V. Soldatov and J.A. Ripmeester: *Chem. Mater.* **12**, 1827 (2000).
12. O. Kristiansson and L.E. Terenius: *J. Chem. Soc., Dalton Trans.* 1415 (2001).
13. I. Kim, B. Kwak, and M.S. Lah: *Inorg. Chim. Acta* **317**, 12 (2001).
14. A.V. Nossov, D.V. Soldatov, and J.A. Ripmeester: *J. Am. Chem. Soc.* **123**, 3563 (2001).
15. D.V. Soldatov and J.A. Ripmeester: *Chem. Eur. J.* **7**, 2979 (2001).
16. D.V. Soldatov and J.A. Ripmeester: *Stud. Surf. Sci. Catal.* **141**, 353 (2002).
17. D.V. Soldatov, E.V. Grachev, and J.A. Ripmeester: *Cryst. Growth Des.* **2**, 401 (2002).
18. T. Ueda, T. Eguchi, N. Nakamura, and R.E. Wasylshen: *J. Phys. Chem. B* **107**, 180 (2003).
19. Yu.Yu. Enakieva, Yu.G. Gorbunova, L.I. Demina, and A.Yu. Tsvadze: *Zh. Neorg. Khim.* **48**, 1986 (2003).
20. D.V. Soldatov, A.S. Zanina, G.D. Enright, C.I. Ratcliffe, and J.A. Ripmeester: *Cryst. Growth Des.* **3**, 1005 (2003).
21. D.V. Soldatov: *J. Inclusion Phenom.* **48**, 3 (2004).
22. N.G. Parsonage and L.A.K. Staveley: In J.L. Atwood, J.E.D. Davies, and D.D. MacNicol (eds.), *Inclusion Compounds*, Vol. 3, Academic Press, London (1984), pp. 1–36.
23. E.A. Ukraintseva, Yu.A. Dyadin, N.V. Kislykh, V.A. Logvinenko, and D.V. Soldatov: *J. Inclusion Phenom.* **23**, 23 (1995).
24. A. Sopková, T. Wadsten, J. Bubanc, and M. Reháková: *J. Thermal Anal.* **56**, 1359 (1999).
25. D.V. Soldatov, V.A. Logvinenko, and Yu.A. Dyadin: *Russ. J. Inorg. Chem.* **40**, 309 (1995).

26. D.V. Soldatov, J. Lipkowski, and E.V. Grachev: *J. Struct. Chem.* **36**, 830 (1995).
27. D.V. Soldatov and J. Lipkowski: *J. Struct. Chem.* **36**, 979 (1995).
28. D.V. Soldatov and J. Lipkowski: *J. Struct. Chem.* **36**, 983 (1995).
29. Yu.A. Dyadin, D.V. Soldatov, V.A. Logvinenko, and J. Lipkowski: *J. Coord. Chem.* **37**, 63 (1996).
30. D.V. Soldatov, Yu.A. Dyadin, E.A. Ukraintseva, B.A. Kolesov, and V.A. Logvinenko: *J. Inclusion Phenom.* **26**, 269 (1996).
31. D.V. Soldatov, Yu.A. Dyadin, J. Lipkowski, and A.G. Ogienko: *Mendeleev Commun.*, 11 (1997).
32. E.A. Ukraintseva, D.V. Soldatov, and Yu.A. Dyadin: *Russ. J. Inorg. Chem.* **42**, 283 (1997).
33. D.V. Soldatov, B.A. Kolesov, J. Lipkowski, and Yu.A. Dyadin: *J. Struct. Chem.* **38**, 819 (1997).
34. D.V. Soldatov and J. Lipkowski: *J. Struct. Chem.* **39**, 238 (1998).
35. D.V. Soldatov and J. Lipkowski: *J. Inclusion Phenom.* **30**, 99 (1998).
36. D.V. Soldatov and J.A. Ripmeester: *Supramol. Chem.* **9**, 175 (1998).
37. E.A. Ukraintseva, D.V. Soldatov, Yu.A. Dyadin, V.A. Logvinenko, and E.V. Grachev: *Mendeleev Commun.*, 123 (1999).
38. D.V. Soldatov, V.A. Logvinenko, Yu.A. Dyadin, J. Lipkowski, and K. Suwinska: *J. Struct. Chem.* **40**, 757 (1999).
39. V.A. Logvinenko and D.V. Soldatov: *J. Thermal Anal.* **56**, 485 (1999).
40. D.V. Soldatov, E.A. Ukraintseva, V.A. Logvinenko, Yu.A. Dyadin, E.V. Grachev, and A.Yu. Manakov: *Supramol. Chem.* **12**, 237 (2000).
41. D.V. Soldatov, G.D. Enright, J.A. Ripmeester, J. Lipkowski, and E.A. Ukraintseva: *J. Supramol. Chem.* **1**, 245 (2001).
42. E.A. Ukraintseva, D.V. Soldatov, Yu.A. Dyadin, P.S. Galkin, and A.N. Mikheev: *Russ. J. Phys. Chem.* **77**, 1759 (2003).
43. E.A. Ukraintseva, D.V. Soldatov, and Yu.A. Dyadin: *J. Inclusion Phenom.* **48**, 19 (2004).
44. D. Grdenic, B. Kamenar, and A. Hergold-Brundic: *Cryst. Struct. Commun.* **7**, 165 (1978).
45. D. Grdenic, B. Kamenar, and A. Hergold-Brundic: *Cryst. Struct. Commun.* **7**, 245 (1978).
46. H.B. Buerger, E. Fischer, R.W. Kunz, M. Parvez, and P.S. Progosin: *Inorg. Chem.* **21**, 1246 (1982).
47. E.C. Alyea, S.A. Dias, G. Ferguson, and P.Y. Siew: *Can. J. Chem.* **61**, 257 (1983).
48. D. Grdenic, M. Sikirica, and B. Korpar-Colig: *Croat. Chem. Acta* **62**, 27 (1989).
49. L.N. Ito, A.M.P. Felicissimo, and L.H. Pignolet: *Inorg. Chem.* **30**, 387 (1991).
50. M. Krumm, E. Zagrando, L. Randaccio, S. Menzer, A. Danzmann, D. Holthenrich, and B. Lippert: *Inorg. Chem.* **32**, 2183 (1993).
51. K.A. Byriel, L.R. Gahan, C.H.L. Kennard, and C.J. Sunderland: *J. Chem. Soc., Dalton Trans.* 625 (1993).
52. M.D. Lumsden, K. Eichele, R.E. Wasilishen, T.S. Cameron, and J.F. Britten: *J. Am. Chem. Soc.* **116**, 11129 (1994).
53. S. Afshar, S.T. Marcus, L.R. Gahan, and T.W. Hambley: *Aust. J. Chem.* **52**, 1 (1999).
54. S.T. Marcus, P.V. Bernhardt, L. Grondahl, and L.R. Gahan: *Polyhedron* **18**, 3451 (1999).
55. S.T. Marcus, L.R. Gahan, and P.V. Bernhardt: *Acta Cryst.* **C56**, 655 (2000).
56. C. Kimblin, V.J. Murphy, T. Hascall, B.M. Bridgewater, J.B. Bonanno, and G. Parkin: *Inorg. Chem.* **39**, 967 (2000).
57. V.Yu. Komarov, M.Sc. Theses, Novosibirsk State University, 2001.
58. A.V. Suvorov: *Termodinamicheskaya khimiya paroobraznogo sostoyaniya. Tenzimetricheskiye issledovaniya geterogennykh ravnovesij*, Khimiya, Leningrad (1970) (in Russian), pp. 46–51.
59. V.B. Lazarev, J.H. Greenberg, and B.A. Popovkin: *Curr. Top. Mater. Sci.* **1**, 657 (1978).
60. Z. Otowinowski and W. Minor: *Meth. Enzymol.* **276**, 307 (1997).
61. S. Mackay, W. Dong, C. Edwards, A. Henderson, C. Gilmore, N. Stewart, K. Shankland, and A. Donald: *Maxus, Comprehensive Crystallography Software, Version 4.0*, University of Glasgow, Glasgow (1999).
62. G.M. Sheldrick: *SHELXTL PC, Ver. 4.1 An Integrated System for Solving, Refining, and Displaying Crystal Structure from Diffraction Data*; Siemens Analytical X-ray Instruments, Inc., Madison (1990).
63. G.R. Desiraju: *Acc. Chem. Res.* **24**, 290 (1991).
64. J. Halfpenny and R.W.H. Small: *Acta Cryst.* **B34**, 3758 (1978).
65. R. Åkesson, M. Sandström, C. Stålhandske, and I. Persson: *Acta Chem. Scand.* **45**, 165 (1991).
66. C.G. Jackson: *J. Chem. Soc.* **99**, 1066 (1911).